Přírodovědecká fakulta
Faculty of Science

Jihočeská univerzita v Českých Budějovicích
University of South Bohemia in České Budějovice

Department of Molecular Biology

Characterization of mitochondrial proteins in *Trypanosoma brucei*

Bachelor Thesis

Laboratory of Molecular Biology of Protists Institute of Parasitology
České Budějovice, 2018

Lucia Svoboda

Supervisor: Priscila Peña-Diaz, Ph.D.

Co-Supervisor: Prof. RNDr. Julius Lukeš, CSc

Svoboda, L., 2018: Characterization of mitochondrial proteins in *Trypanosoma brucei*. BSc. Thesis, in English, - 30 p., Faculty of Science, University of South Bohemia, České Budějovice, Czech Republic.

Annotation

In this thesis proteins Tb927.2.3030 and Tb927.11.4870 are localized by in-situ tagging, immunofluorescence microscopy and cell fractionation. Their essentiality for growth is determined by downregulation with RNA interference.

Affirmation

I hereby declare that I have worked on the submitted bachelor thesis independently and used only the sources listed in the bibliography.

I hereby declare that, in accordance with Article 47b of Act No. 111/1998 in the valid wording, I agree with the publication of my bachelor thesis, in full form to be kept in the Faculty of Science archive, in electronic form in publicly accessible part of the STAG database operated by the University of South Bohemia in České Budějovice accessible through its web pages.

Further, I agree to the electronic publication of the comments of my supervisor and thesis opponents and the record of the proceedings and results of the thesis defense in accordance with aforementioned Act No. 111/1998. I also agree to the comparison of the text with the Thesis.cz thesis database operated by the National Registry of University Theses and a plagiarism detection system.

Lucia Svoboda
České Budějovice, 14.5.2018

Acknowledgement

I would like to thank Priscila Peña-Diaz for her great guidance, supervision in both the practical work and the writing and for being a great role model. A big thank you to Prof. RNDr. Julius Lukeš, CSc for giving me the opportunity to work in his amazing laboratory and giving me the motivation to continue my journey into molecular biology. And of course, a thank you to my colleagues, who made the stay in České Budějovice not only productive but also enjoyable.

Abbreviations:

cAMP	cyclic adenosine monophosphate
DNA	desoxy ribo nucleic acid
HAT	Human african trypanosomiasis
HBBS	Hanks‘ balanced salt solution
Hsp	Heat shock protein
kDNA	kinetoplast DNA
LB	lysogeny broth
lhRNAi	long hairpin RNAi
mNG	mNeonGreen
mRNA	messenger RNA
PBS	phosphate buffered saline
PCR	polymerase chain reaction
PQC	protein quality control
RISC	RNA induced silencing complex
RNA	ribonuleic acid
RNAi	RNA interference
rRNA	ribosomal RNA
SDS	Sodium dodecyl sulphate
siRNA	small interfering RNA
Tet	Tetracycline
VSG	variable surface glycoprotein

Table of Content

1. Introduction

Trypanosomatids are flagellated protists of the class Kinetoplastida. They are evolutionary successful parasites found in all groups of vertebrae, several invertebrae and plant hosts, all over the planet. Common pathogens of tropical diseases in human as well as livestock are *Trypanosoma brucei* (African sleeping sickness), *Trypanosoma cruzi* (Chagas disease) and members of the genus *Leishmania* (distinct forms of leishmaniasis worldwide) (Lopes, 2010).

Trypanosoma brucei is the causative agent of African trypanosomiasis, responsible for 3 million deaths of cattle and 70 000 new infections in humans every year. The metacyclic parasites are transmitted by the bite of the tsetse fly. In the skin lesion, the trypanosome transforms into bloodstream form, travel through the body and replicate by binary fission. Within a few weeks, they can invade the central nervous system. Tsetse flies are infected, when they bite a host of trypanosomatids. The parasites transform into procyclic trypomastigotes in the flies gut, passage then to epimastigote form in the flies midgut and complete the cycle by transformation into metacyclic trypomastigotes in the salivary gland of the fly (Figure 1)(Lopes, 2010).

Trypanosoma brucei brucei causes Nagana in cattle. About 98% of all cases of human African trypanosomiasis (HAT) are caused by *Trypanosoma brucei gambiense*, another sub-specie of *Trypanosoma brucei* (Babokhov et al., 2013). These are characterized as HAT chronic infections; the remaining 2% are acute infections caused by *Trypanosoma brucei rhodesiense.* Even though infections have been on a downwards trend, HAT still affects 50 000-70 000 people in endemic areas. In the first stage of the human disease, the parasite has not yet invaded the central nervous system. The parasites evade the immune response by continuously switching their variable surface glycoprotein (VSG) coat in a process called antigenic variation. The immune system of the host cannot recognize the changing VSG of the parasite and gets exhausted as a result. Common symptoms of the early stage include fever, headaches, pain in the joints and swelling of the insect bite. In the second stage of the infection, the parasite has crossed the blood-brain barrier and entered the central nervous system. The eponymous symptoms of the later stage are disruption of the circadian rhythm resulting in irregular sleeping/wakeness patterns, along with other symptoms like confusion and poor coordination, tremors, general motor weaknesses, irritability and aggressive behavior. HAT is fatal if not treated in the early stage (Babokhov et al., 2013).

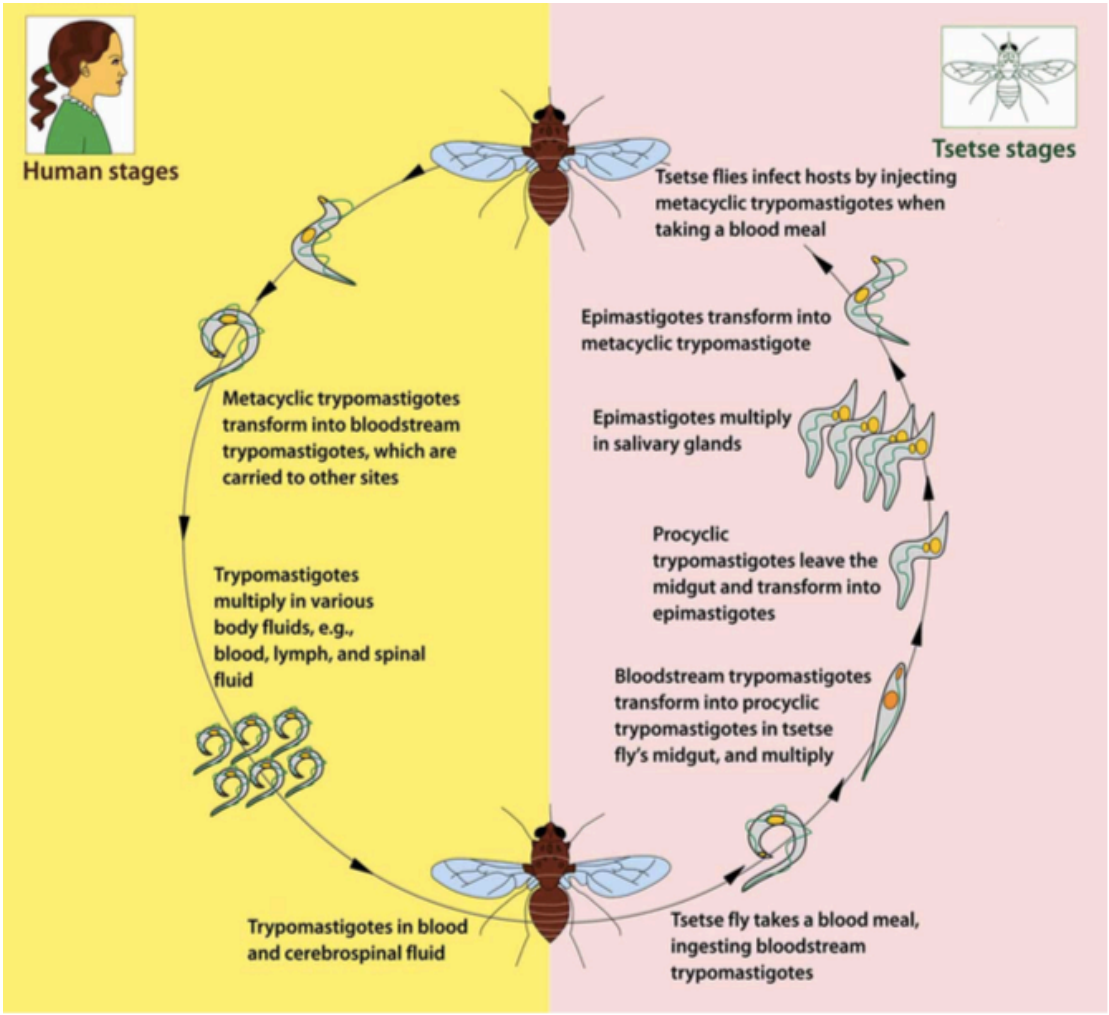

Figure 1: Transmission cycle of *Trypanosoma brucei*. During a blood meal on the mammalian host, an infected tsetse fly (genus *Glossina*) metacyclic trypomastigotes are transferred into the skin tissue. The parasites enter the bloodstream through the lymphatic system. Inside the host, they transform into bloodstream trypomastigotes, are carried to other sites and blood fluids (e.g., lymph, spinal fluid) throughout the body and continue the replication by binary fission. The tsetse fly becomes infected with bloodstream trypomastigotes when taking a blood meal on an infected mammalian host. In the fly's midgut, the parasites transform into procyclic trypomastigotes, multiply by binary fission, leave the midgut and transform into epimastigotes. The epimastigotes reach the fly's salivary glands and continue multiplication by binary fission. The entire life cycle of African trypanosomes is represented by extracellular stages. Adapted from (Lopes, 2010)

Trypanosoma contain unique organelles. In trypanosomes the site of glycolysis is located in a modified peroxisome, the glycosome. It is a spherical structure, with a protein-rich matrix, surrounded by a phospholipid bilayer, but lacking DNA. Glycosomes harbour the first 6-7 enzymes of the glycolytic pathway. The glycolysis starts in the peroxisomes and is continued in the cytoplasm. Glycerol-3-phosphate used in the process is replenished in the mitochondria in the bloodstream form. (Parsons, 2004).

Trypanosomatids possess a single ramified mitochondrion. Mitochondria of trypanosomes contain an unusual amount of mitochondrial DNA, known as kinetoplast DNA (kDNA). It is a disk-shaped network consisting of several thousand minicircles, linked together like medieval chainmail, and a few dozen maxicircles (Verner et al., 2015). The volume and activity of the mitochondrion depends on the environmental conditions. It is the most active in the midgut of the host, where glucose levels are low and least active in the blood, where glucose levels are high (Lopes, 2010).

Because of its unique features and pathogenicity, *T. brucei* is a well-established model organism (Lopes, 2010).

Trypanosoma brucei possess a stressful life cycle in which they go through a lot of morphological changes and are exposed to harsh environments. Factors like change in pH and temperature, oxygen and nutrient deficiency put stress on the cells. In order to ensure proper function of cell organelles, the cells have to have a protein quality control system.

Maintenance of protein functionality and concentration in the cell is a tightly governed process. As proteins are present in cells in very high concentration, all protein-protein interactions have to be strictly regulated. Chaperones and proteases ensure protein homeostasis - and not only when temperature, pH, nutrient availability or pathogens put stress on the cells and have to be removed by regulated proteolysis. This protein control system regulates protein synthesis, folding, unfolding, and turnover. While some chaperones assist folding of newly synthesized polypeptides or the transit across membranes, other ATP-dependent proteases actively unfold proteins at the expense of ATP (Requena et al., 2015).

Different organisms and cellular compartments depend on different systems to control protein homeostasis. In the cytoplasm of eukaryotes, ubiquitin-proteasome system is the main pathway of protein degradation. Target proteins are tagged with several copies of ubiquitin, which targets the protein to the proteasome (Amm et al., 2014). It is a large, barrel-shaped, ATP-dependent protease complex in which the protein is degraded. Many proteins located in the cytoplasm, nucleus, endoplasmic reticulum and outer membrane of the mitochondria are degraded by the proteasome pathway. However, the chloroplast, mitochondria and peroxisomes also contain unique system ensuring protein quality control (Dougan, 2013).

ATP-dependent Clp proteases are highly conserved among bacteria and in chloroplasts and mitochondria of eukaryotes (Dougan, 2013). They belong to the superfamily of AAA+ proteins, which usually form an oligomeric ring structure of usually six monomers (Requena et

al., 2015). They participate in a variety of different processes, namely protein folding, activation and disaggregation. General and regulated proteolysis both require Clp. General proteolysis removes damaged proteins from the cell in the process of homeostasis (Dougan, 2013).

Proteins that fail to fold properly, but escape the proteasome pathway, commonly fold aggregates. Disassembly of these aggregates is mediated by a group of members of the AAA+ family (Hanson and Whiteheart, 2005). Important member of this family are Hsp104 and Hsp78 in yeast and their ortholog ClpB in bacteria. Disaggregation and reactivation of aggregated proteins is usually favored over proteolysis, as it requires less energy expenditure to refold a protein than to synthesize a new polypeptide chain (Liberek et al., 2008).

The unfoldase ClpB is part of the protein quality control network in *E. coli*. It unfolds and resolubilizes protein aggregates. Working together with Hsp70/DnaK chaperones it actively solubilizes and refolds protein aggregates (Figure 2). ClpB and other related AAA+ proteases usually consist of an N-terminal domain and two ATP-binding domains. Furthermore, they contain a highly conserved loop at their central pore, which cause conformational changes when they come in contact with substrate protein. Together with ATP binding, this results in ratchet-like movements, pulling the protein through the central pore of the protease and unfolding it (Dougan, 2013).

The model eukaryote yeast, *Saccharomyces cerevisiae* contains two homologs of bacterial ClpB. Hsp104 is compartmentalized in the cytosol, while Hsp78 is targeted towards the mitochondria (Erives and Fassler, 2015, Matthias Schmitt, 1996). They recover polypeptides from aggregates, especially after heat stress. Hsp104 cooperates with Hsp70 and Hsp40 to reactivate proteins that have become unfolded and aggregated (Glover and Lindquist, 1998). Hsp78 together with mtHsp70 and Pim1 work as the protein quality control system of the mitochondrial matrix in *Saccharomyces cerevisiae* (Bender et al., 2011).

In plants ClpB/Hsp100 is present in the cytoplasm, mitochondria and chloroplast (Singh et al., 2010, Singh and Grover, 2010). In animals, ClpB disaggregases Hsp78 and Hsp104 are not detectable. It is hypothesized that the evolution of multicellularity that led to the loss of some biosynthetic pathways, also lead to a secondary loss of the chaperones (Erives and Fassler, 2015).

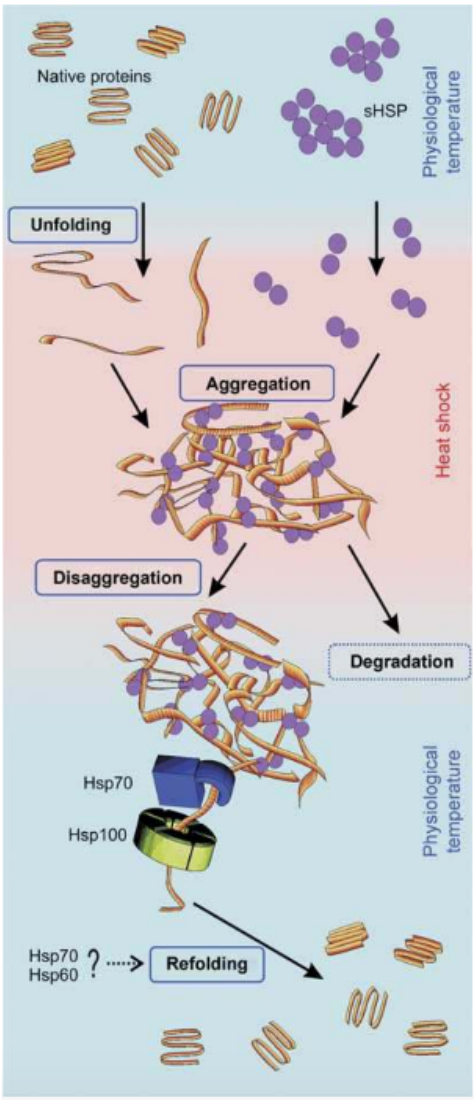

Figure 2: As a result of stress, native proteins unfold. With the help of small heat shock proteins (sHSP), aggregates form. Aggregates are entangled by Hsp70, unfolded by ClpB /Hsp100 and refolded by chaperones or degraded. Adapted from (Liberek et al., 2008)

There are at least two mammal AAA+ proteases that share structural and functional features with ClpB/Hsp100, called p47/CDC48 and torsin A, which are involved in the reassembly of the Golgi apparatus and solubilization of protein aggregates respectively (Singh and Grover, 2010, Wang et al., 2004, Caldwell et al., 2003).

An ATP dependent Clp protease subunit, Hsp78 can be found in the trypanosomatid genome database TriTrypDB, under accession number Tb927.2.3030 (Aslett et al., 2010). TrypTag, an online resource, aiming to provide localization of every gene encoded in *T. brucei,* predicts the localization of the protein in the mitochondria (Dean et al., 2017). In the TrypTag project, fluorescent protein tagging by long primer PCR is used to localize hundreds of proteins. Proteins with an annotated signal peptide are tagged at the C-terminus, all other peptides at the

C- and N-terminus. The data is available at TrypTag website, TriTrypDB and will be available as raw data via a FTP server (Figure 4) (Dean et al., 2017)

Endogenous tagging is the modification of the target gene sequence to code for a recognizable polypeptide, called a tag (Dean et al., 2015). The sequence for the tag can be inserted into the genome of the protist, at either terminus of a gene or in the middle of a gene by homologous recombination. In order for recombination to take place, the sequence has to contain at least 50-100 nucleotides homology. The construct is generated by PCR amplification with long primers, that will amplify the region of targeting, which will flank a cassette that contains the tag and an antibiotic resistance gene (Figure 3). Successful recombinant clones are selected using antibiotic resistance (Arhin et al., 2004, Dean et al., 2017, Dean et al., 2015).

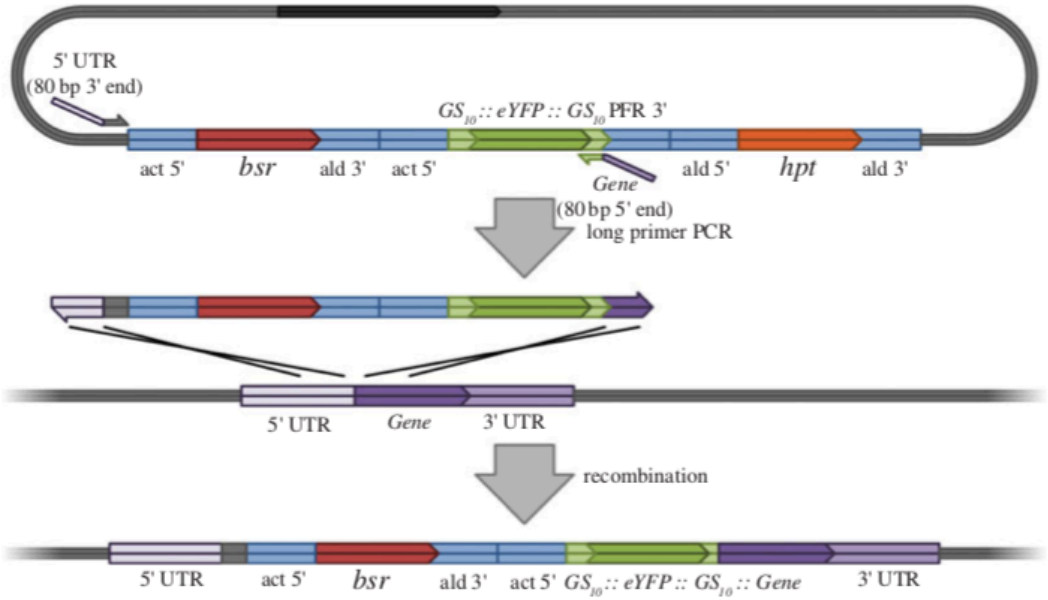

Figure 3: Schematic representation of in-situ tagging with long primer PCR constructs. A cassette containing the tag and an antibiotic resistance gene are amplified with primers containing a homologous sequence with the target gene. It is integrated into the sequence of the target gene by homologous recombination. Adapted from (Dean et al., 2015)

To test the preliminary result of TrypTag localizing Tb927.2.3030 in the mitochondria, we in-situ tagged it using the long primer PCR approach with the pPOTv4 plasmid, in which YFP was replaced by V5 (Peña-Diaz et al., 2017).

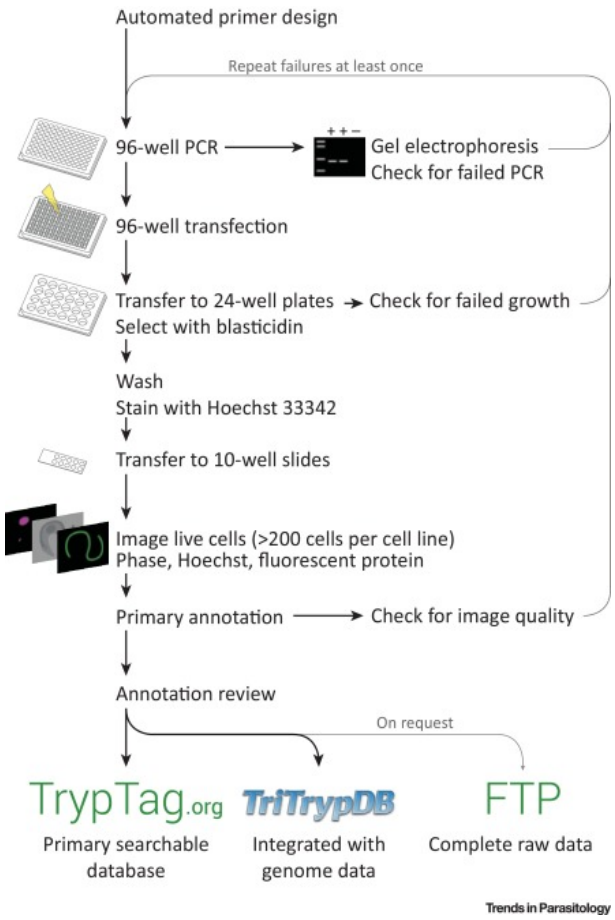

Figure 4: Schematic representation of the High-Throughput Protein Tagging Workflow of the TrypTag project. Adapted from (Dean et al., 2017)

To study the essentiality and function of our gene of interest, RNAi was used. RNAi is a natural defense mechanism against RNA viruses in cells, stabilize the DNA by silencing mobile parts and regulate protein synthesis. RNA interference was first reported in *Caenorhabditis elegans*, where double stranded RNA lead to mRNA degradation and phenotypes. Shortly after, the mRNA degradation induced by RNAi was documented in many other organisms, including trypanosomes (Wang et al., 2000, Ngô et al., 1998). When double stranded RNA is present in cells it gets cleaved in 21-23 nucleotide sequences, called small interfering RNA (siRNA), by the ribonuclease III-like nuclease Dicer. The antisense strand gets loaded into the large RISC (RNA-induced silencing complex) complex. The siRNA targets the RISC to the complementary mRNA, which is subsequently cleaved and degraded (AB, 2014).

RNAi has been used in *T. brucei* to study genes, using a tetracycline suppressor system to induce expression. Long hairpin RNAi (lhRNAi) is now preferred over plasmids flanking T7 promoters and tetracycline suppressors (Dean et al., 2015). The plasmid bears a T7 promoter and two repeats of the target region flanking with a stuffer region between them (Figure 5).

Addition of tetracyclin induces expression of the reverse complement sequence of the genes of interest, and the resulting mRNA anneals to form a double stranded RNAi, resembling a hairpin. This allows a quick loss-of-function screen of genes and from there an implication of the necessity and function (Michael R. McAllaster, 2016).

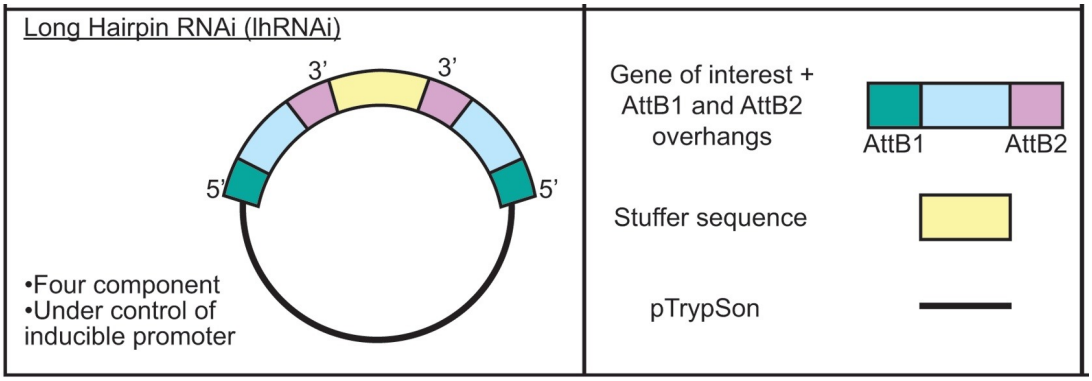

Figure 5: Schematic representation of lhRNAi, assembled by Gibson assembly and components comprising the structure. Adapted from (McAllaster et al., 2016)

Gibson assembly can be used to construct the lhRNAi vector, to study the essentiality of proteins for cell growth. Gibson assembly is a one-step isothermal process that rapidly assembles multiple DNA segments with in a single reaction. Three enzymes are used to anneal the overlapping overhangs of the DNA segments (Gibson et al., 2009). A 5'exonuclease exposes the overhanging sequences for specific annealing of the complimentary end of the other DNA segments, a DNA polymerase extends the missing overhangs behind overlapping regions and DNA ligase fills in the nicks between segments. The 15-20 base pairs of homologous sequence are encoded by non-annealing overhangs of the PCR primers (Figure 6) (McAllaster et al., 2016, Gibson et al., 2009).

All experiments were also performed on protein Tb927.11.4870, which does not have any well-known homologs. Differences in patterns of localization are found and discussed.

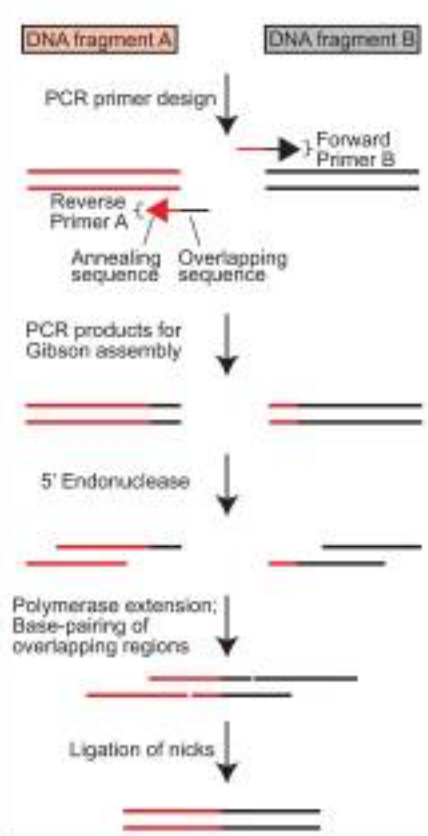

Figure 6: Schematic representation of the construction of RNAi plasmids by Gibson assembly. Adapted from (McAllaster et al., 2016)

2. Aim of the thesis

The aim of the thesis was the characterization of genes Tb927.11.4870 (p4870) and Tb927.2.3030 (p3030) in the procyclic form of *Trypanosoma brucei*, using RNAi to determine essentiality, as well localization analysis via immunofluorescence assay and crude cell fractionation of genes tagged in-situ with V5 tag.

3. Materials and Methods

3.1. Generation of constructs and cassettes for trypanosome transformation

3.1.1. Cell lines

For the amplification of DNA plasmids, *Escherichia coli* XL1-Blue was used.

All experiments were performed procyclic SmoxP9 in *Trypanosoma brucei.* They were cultivated at 27°C in SDM79 medium supplemented with 7.5 mg/L hemin and 10% fetal calf serum (FCS) in presence of puromycin (0.5 µg/mL) to ensure the stable expression of T7 polymerase and tetracycline repressor.

3.1.2. Construction of RNAi plasmids

For the construction of the RNAi cell lines by Gibson assembly the TbPLK pTrypSon plasmid was used (McAllaster et al., 2016). Two PCR amplified regions (primers see Table 1) were cloned in the vector between *Hind*III and *Xho*I restriction sites, with a 535bp long AttB2 and stuffer region between them.

Linearized pTrypSon vector backbone, PCR-generated stuffer and target region fragments (all gel extracted with NucleoSpin Gel and PCR clean-up kit, Macherey-Nagel) were mixed with a 2x Gibson assembly master mix (699 µL water, 320 µL 5 x isothermal reaction buffer (500 mM Tris- Cl, pH 7.5, 250 mg/mL PEG-8000, 50 mM $MgCl_2$, 50 mM DTT, 1 mM each of four dNTPs, 5 mM beta-NAD), 0.64 µL T5 Exonuclease (Epi- centre, 10 U/µL), 20 µL Phusion DNA polymerase (NEB, 2 U/µL) and 160 µL Taq DNA ligase (NEB, 40 U/µL)) and incubated at 37°C for 1 hour.

The assembly mixture was transformed into chemically competent *E. coli XL1-Blue*. Successful clones were selected by 25 µg/mL ampicillin and screened by colony PCR; positives were subsequently grown into LB in presence of 25 µg/mL ampicillin for plasmid DNA miniprep-aration (Macherey-Nagel, NucleoSpin Plasmid). The correct vector assembly was verified by sequencing with primers for the target sequence.

The construct was linearized with 10 units *Not*I-HF and transfected in SMOXP9 *T. brucei* cells.

Table 1: For the construction of long hairpin RNAi long primers were designed

Name	Sequence
p3030 fw	ACAAGTTTGTACAAAAAAGCAGGCTAAGCTT GGCTCTTTAGTT-GCTGGTGC
p3030 rv	ACCACTTTGTACAAGAAAGCTGGGTCTCGAGCTTTAGGCG-GACAAGCTCAC
p4870 fw	ACAAGTTTGTACAAAAAAGCAGGCTAAGCTT GAACTCGAAATGGGGCATAA
p4870 rv	ACCACTTTGTACAAGAAA-GCTGGGTCTCGAGGTGACATGGACTCGATGGTG

3.1.3. Construction of tagged cell lines

For the construction of in situ tagged cell lines the long-primer PCR approach was used. p4870 and p3030 were tagged at their C- and N-terminus with V5 in separate cell lines. To amplify the PCR product a pPOTv4 vector, in which the yellow fluorescent protein was replaced with a V5 tag, was used (primers see table 2). The PCR product was transfected into procyclic *T. brucei* SMOXP9 cells (Dean et al., 2015).

Table 2: For the generation of tagged cell lines primers were designed:

Name	**sequence**
N-terminal tagged p4870 fw	AGGACTTGCTTCTTGTACAGTATTTGGGCGG-GAATAAAACTCTTGTATCAGAATTAGGTAAC-GTGAGCTGTAGTGCACTAgtataatgcagacctgctgc
N-terminal tagged p4870 rv	ATGCGCGTTTCTAAGGCCAGGTCCCACATC-CATTGCGGTTGCTCCCTCCCTGT-GAAAAGCTTGTAAATTCTACCGGACATactacccgatcctgatcc
C-terminal tagged p4870 fw	TCCCCCCGAACTGTCGCACCCCACCGCCTCCT-GAGGCACCATCGAGTCCATGTCA-CATCTCAGCTATCCCTAAATCGTAGggttctggtagtggttcc
C-terminal tagged p4870 rv	ACCCCTCTCCTGCGGCCGTTCCATCATCATCAG CCATACCTTCTCCCTGGA-GACTAATGGAAACAAGAAAGGAG-TCAACCccaatttgagagacctgtgc

Name	sequence
N-terminal tagged p3030 fw	ATCAAGGAGTCAACTGACAAAG-GTATTCCTACCGCTGAAACTGAC-GAAAAAAAAAGAGGGA-GACAAAATAAGCCGAAAGGgtataatgcagacctgctgc
N-terminal tagged p3030 rv	TAGCCCCCGACCTGCACGGTAC-GTTTTGTCGTCAAGCTGTTTGCCCACACACCAC-GGCCAC-CCGAACCCAGCTTTCGCATactacccgatcctgatcc
C-terminal tagged p3030 fw	GAGAGGTATTTGTGCATCAGAACCAT-GACGCCGTGCGCCCAGTGGATGCCGCA-GACCTGGG-TCCGCAACTCACAGAATGAggttctggtagtggttcc
C-terminal tagged p3030 rv	CTAGTGATGAT-CCTGTTTTGTTTTGTTTTGTTTTTTTTTGCAAT-CAAGTCTT-CCTTTTATGTAGGAGGAAGGTGACAGGTccaatttg agagacctgtgc

3.1.4. Transfection

Transfections were performed according to a well-established protocol (Wang et al., 2000). 2 x 10^7 cells were harvested by centrifugation at 800 x*g* for 10 minutes and resuspended in 100 µL Amaxa Human T Cell Nucleofector Solution and Supplement (Lonza, Amaxa Human T Cell Nucleofector Kit), containing either PCR product or 10 µg of linearized vector. The mixture was loaded in a 2-mm electroporation cuvette and transfection was carried out using an AMAXA Nucleofector 2b, applying the program X-014. The cells were immediately allowed to recover in 10 mL fresh SDM-79 for 18 hours. After recovery, the appropriate antibiotic for selection was added, the culture was serial diluted in a 24-well plate and the cells were grown for 10 days to allow clones to establish in culture.

3.1.5. Selection

Cell lines containing the RNAi vector were selected using phleomycin (2.5 µg/mL) and induced with tetracycline (1 µg/mL) to observe RNAi effect. V5-tagged (in-situ) cell lines with at the C-terminus were selected with hygromycin (50 µg/mL). N-terminus V5-tagged cell lines were selected using blasticidin (10µg/mL) (summary of antibiotic concentration used see table 3)

Table 3: Concentrations of antibiotics used

Antibiotic	Concentration
Phleomycin	2.5 µg/mL
Tetracyclin	1 µg/mL
Hygromycin	50 µg/mL
Blasticidin	10 µg/mL

3.2. Western blot

Cells were counted and harvested by spinning at 1800 xg for 10 minutes. The pellet was re-suspended in LDS buffer to reach a concentration of $5x10^5$ cells/µL. DTT was added to a final concentration of 0,05 M. The samples were cooked at 98°C for 10 minutes and sheared. $5x10^6$ cells or 10µL of each sample were loaded on to SDS-page gel and blotted on a PVF membrane. The membrane was blocked with 5% non-fat milk in PBS for 1 hour. It was probed with 1:2000 dilution of monoclonal mouse anti-V5 antibodies overnight. After subsequent washing with PBS-tween, the membrane was probed with anti-mouse antibodies 1:2000 conjugated to horseradish peroxidase for 1-2 hours. Following thorough washing, the protein was visualized with Bio Rad, Clarity ECL Western Substrate.

3.3. Immunofluorescence and DAPI staining

In-situ tagged cell lines were observed by immunofluorescence analysis (Peña-Diaz et al., 2017). 10^7 cells were incubated with 0,2 µmol MitoTracker Red for 20 minutes, centrifuged at 1800 xg for 10 minutes and fixed in 4% (w/v) paraformaldehyde solution in phosphate buffered saline (PBS) for 18 minutes. After 2-minute centrifugation at 1800 xg, the fixative was eliminated and the cells were resuspended in PBS. This solution was placed on microscope slides and cells were allowed to settle on the slide for 30 minutes. The cells were permeabilized with 0.2% (v/v) Triton X-100 solution for 30 minutes, blocked with 0.5% (w/v) PBS/gelatin and probed with anti-V5 antibody in rabbit or mouse, as stated. After thorough washing of the slides, they were probed with secondary antibodies (anti-mouse/ anti-rabbit labeled with FITC). DNA was visualized with ProLong antifade reagent with DAPI (Life Technologies). The immunofluorescence analysis was performed on a Zeiss Axioplan 2 microscope with an Olympus DP73 digital camera, using the Olympus cellSense software. The images were processed using ImageJ.

3.4. Crude cell fractionation

$5x10^8$ mid-log phase cells were harvested by centrifugation at 1000 x*g*, for 10 minutes at 4°C. After washing the pellet two times with cold SHE buffer (250 mM sucrose, 25 mM HEPES, 1 mM EDTA, pH 7,4) the pellet was resuspended in 100µL of said buffer. The concentration of the suspension was determined by Bradford protein assay. Aliquots containing 1 mg of total protein were centrifuged and the pellet was resuspended in 200µL of cold Hanks' balanced salt solution (1,26 mM $CaCl_2$, 5,33 mM KCl, 0,44 mM, KH_2PO_4, 0,81 mM $MgSO_4$, 138 mM NaCl, 4 mM $NaHCO_3$, 0,3 mM Na_2HPO_4, 5,6 mM glucose, pH 7,3) (HBSS) and digitonin was added to a concentration of 0,4 µg/µL. After incubating for 5 minutes on ice, the soluble cytosolic fraction was collected by centrifuging for 2 minutes at 14000 x*g* at 4°C. The pellet was washed with HBSS buffer once and resuspended in 200µL HBSS. Triton X-100 was added to a final concentration of 0,1%(v/v) and incubated for 5 minutes on ice. The mitochondrial fraction was collected by centrifugation at 14000 x*g* for 2 minutes. The pellet containing insoluble proteins was washed with HBSS buffer and resuspended in 200µL HBSS buffer. The fractions were mixed with 2x SDS sample buffer, boiled at 98°C for 10 minutes, sheared as necessary and analyzed by western blot.

4. Results

4.1. Gibson assembly

Long hairpin RNAi was prepared by Gibson assembly as described before (Figure 7). After successful insertion of the target sequences was confirmed by sequencing, a midi prep was prepared and 10 ng of DNA were linearized and transfected (Figure 8) into PCF *T. brucei* SMOXP9 cells.

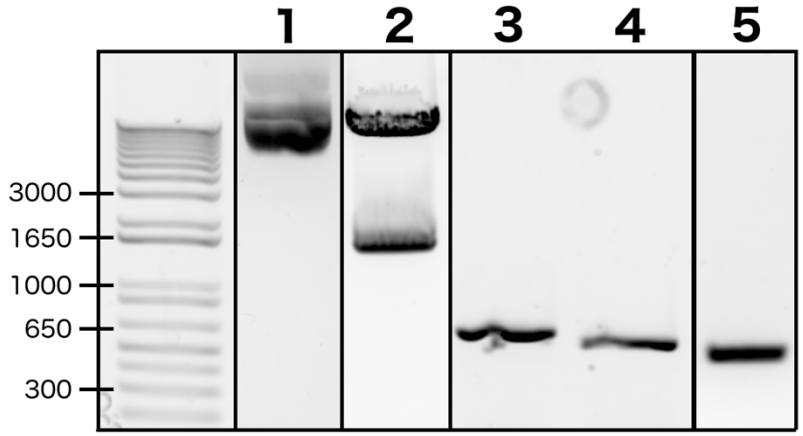

Figure 7. DNA electrophoresis of long hairpin RNAi construct constituents. First lane: 1kb DNA ladder; 1) 0,3 ug pTrypSon plasmid; 2) 5ug pTrypSon plasmid digested with *Hin*dIII, resulting in the release of the TbCentrin-stuffer insert. The linearised vector was gel-extracted and purified 3) p4870 RNAi target region; 4) p3030 RNAi target region; and 5) stuffer, synthesized by PCR with primers shown in table 2

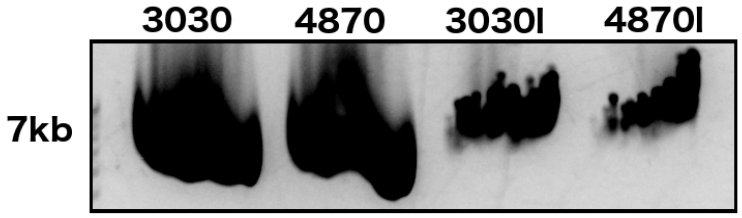

Figure 8: DNA electrophoresis of ready-made RNAi constructs for p3030 and p4870

4.2. In-situ tagging with V5

The cassette to tag p3030 and p4870 with V5 was amplified by PCR using long primers (Dean et al., 2015) (Figure 9). The PCR product was transfected in procyclic *T. brucei* SMOXP9 cells. The successful tagging of p3030 and p4870 was determined by Western blot analysis, shown in Figure 10.

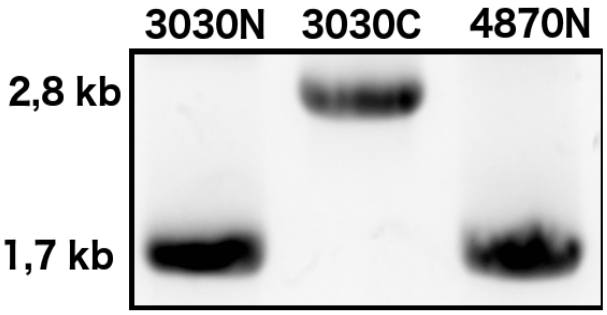

Figure 9. PCR-amplified cassettes obtained using the long primer PCR approach. The pPOTv4v5 vector was used as template to amplify the cassette that will insert an N- and C-terminal V5 tag in the locus of p3030 and an N-terminal V5 tag in the p4870 locus

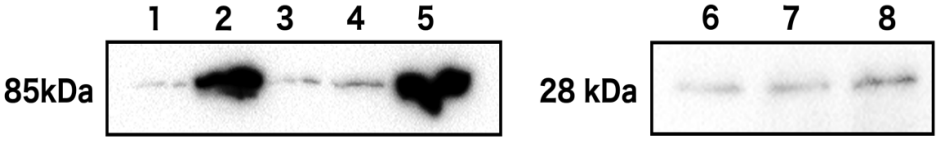

Figure 10. Detection of V5 tag by Western blot for verification of in-situ tagging of the p3030 and p4870. $5x10^6$ cells per well were used. Protein was detected by hybridisation with a monoclonal anti-V5 antibody (Sigma-Aldrich). 1: C-terminal tagged p3030, clone 1; 2: C-terminal tagged p3030, clone 2; 3: N-terminal tagged p3030, clone 1; 4: N-terminal tagged p3030, clone 2; 5: N-terminal tagged p3030, clone 3; 6: N-terminal tagged p4870, clone 1; 7: N-terminal tagged p4870, clone2; 8: N-terminal tagged p4870, clone3

4.3.p4870

4.3.1. Subcellular localization

Preliminary results of life images of N-terminal in-situ tagged p4870 with mNeonGreen (mNG), predicted mitochondrial localization of the proteins (Aslett et al., 2010).

In-situ tagging and immunofluorescence analysis of p4870 with V5 at the C-terminus revealed that the protein is distributed throughout the cell, while showing accumulation at the cell organelles (Figure 11). The western analysis of crude cell fractions supported localization associated to membranes, showing a signal in the insoluble fraction for C-terminal tagged V5 protein. N-terminal tagged cell protein showed a signal in the cytosolic fraction (Figure 12). This is probably due to blockage of an N-terminal signal by the V5 tag.

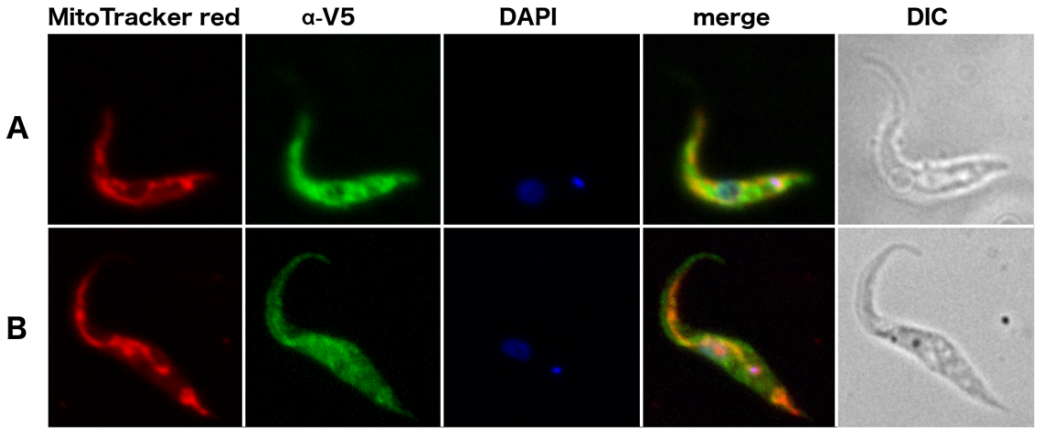

Figure 11: Immunofluorescence analysis of in-situ tagged *T. brucei* PCF cell lines, immunodecorated with anti-V5, after incubation with the mitochondrial dye Mito-tracker Red. DAPI was used to stain DNA. .
A: N-terminal tagged p4870, anti-V5 antibodies in rabbit
B: C-terminal tagged p4870, anti-V5 antibodies in mouse

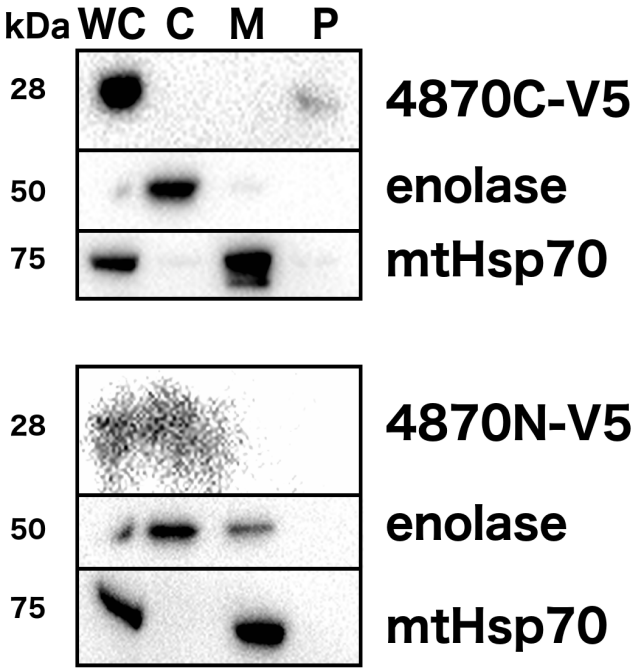

Figure 12: Western blot analysis of crude cell fractionation of C- or N-terminal V5 in-situ tagged cell lines. Whole cell lysate (WC), cytosolic (C), organellar (M) and unsoluble (P) fractions are compared and incubated with anti-mtHsp70, anti-enolase and anti-V5 antibodies. It shows that p4870 is targeted to the cytosol if it is tagged at the N-terminus and found in the unsoluble fraction when tagged at the C-terminus

HHpred predicted the highest similarity of p4870 to various transmembrane proteins, even though the probability was not very high with any protein (Söding, 2005) (Zimmermann et al., 2017). Phobius predicted two transmembrane domains. This is in alignment with the result of

the C-terminal tagged cell lines, localizing p4870 to the membrane-associated fraction (Käll et al., 2007a).

4.3.2. Inducible RNAi expression

Tetracycline-induced and un-induced SMOXP9 cell lines with constructs for RNAi expression were recorded over the course of 7 days. Three clones were assessed for each transfected construct. The cultures were counted every day and diluted with SDM79 media to a concentration of $2x10^6$ cells/mL.

The downregulation of p4870 did not result in any growth phenotype as shown in figure 13.

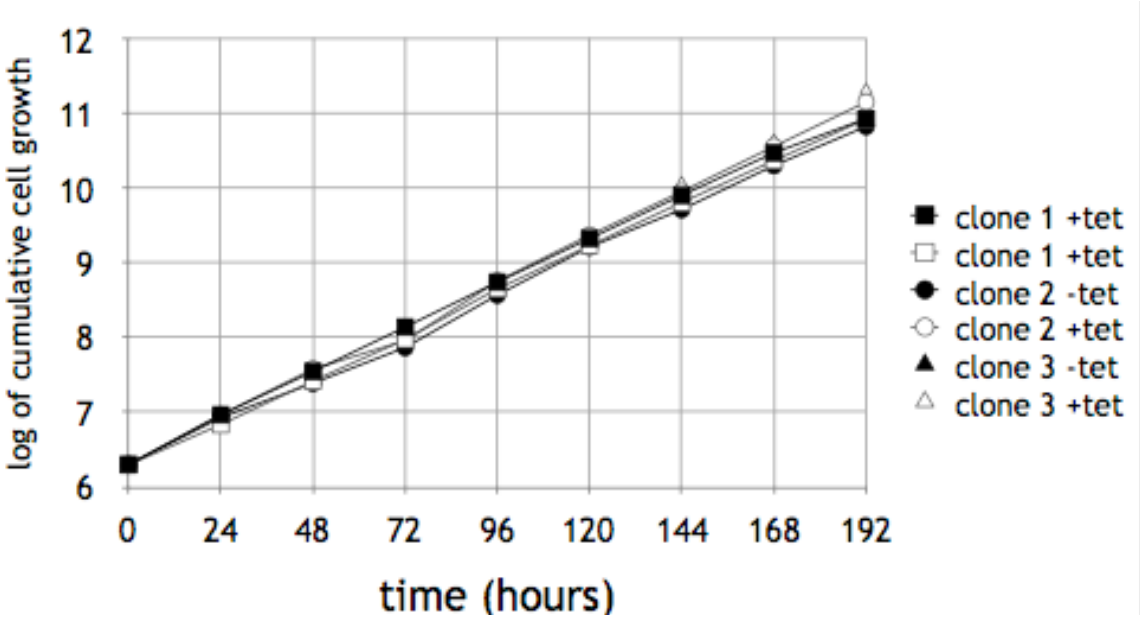

Figure 13. Growth curve of cells transfected with long hairpin RNAi targeting for p4870, comparing non-induced cell lines to cell lines induced with tetracycline

4.4.p3030

4.4.1. Subcellular localization

Preliminary results of life images of N-terminal in-situ tagged p3030 with mNG, predicted mitochondrial localization of the proteins (Aslett et al., 2010).

Prediction of localization of p3030 with bioinformatics softwares was inconclusive. While some programs predicted mitochondrial location (mitoProt (Claros and Vincens, 1996), targetP (Emanuelsson et al., 2000), Phobius (Käll et al., 2007b) and MultiLoc (Hoglund et al., 2006)), other programs did not find a mitochondrial targeting signal (iPSORT (Bannai et al., 2002), SOSUIsignal (Gomi et al., 2004) and SignalP (Petersen et al., 2011)).

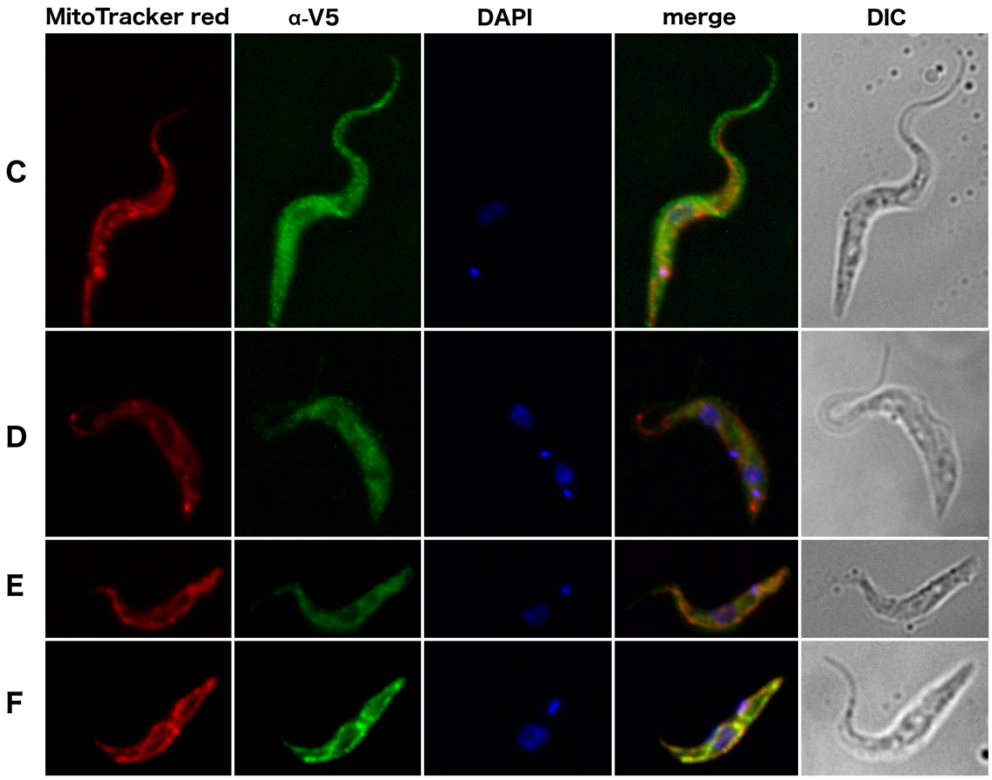

Figure 14: Immunofluorescence analysis of in-situ tagged *T. brucei* PCF cell lines, immunodecorated with anti-V5, after incubation with the mitochondrial dye Mitotracker Red. DAPI was used to stain DNA.
C: N-terminal tagged p3030, anti-V5 antibodies in mouse
D: N-terminal tagged p3030, anti-V5 antibodies in rabbit
E: C-terminal tagged p3030, anti-V5 antibodies in mouse
F: C-terminal tagged p3030, anti-V5 antibodies in rabbit

Immunofluorescence analysis of in-situ tagged p3030 protein showed cytosolic localization with N-terminal tagged cell lines and mitochondrial localization with C-terminal tagged cell

lines (Figure 14). This is in agreement with the western blot analysis of crude cell fractions, which localize C-terminal tagged p3030 to mitochondria and the cytosol, while N-terminal tagged p3030 remained strictly in the cytosol (Figure 15). The marker of mitochondrial compartment, mtHsp70 and the cytosolic marker enolase, were found exclusively in their expected compartments, which ensures a correct separation of the organelles in the fractionation process (Figure 15).

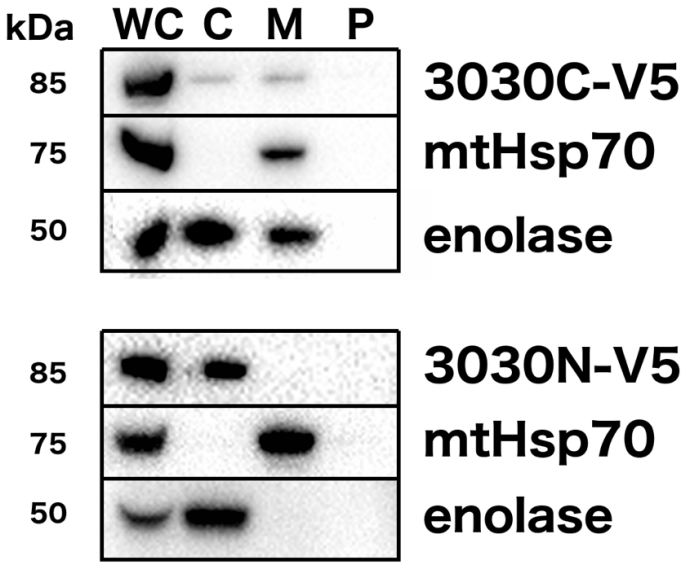

Figure 15: Western blot analysis of crude cell fractionation of C- or N-terminal V5 in-situ tagged cell lines. Whole cell lysate (WC), cytosolic (C), organellar (M) and insoluble (P) fractions are compared and incubated with anti-mtHsp70, anti-enolase and anti-V5 antibodies. It shows that p3030 is targeted to the cytosol if they are tagged at the N-terminus and found in the cytosol as well as the organellar fraction when tagged at the C-terminus

4.4.2. Inducible RNAi expression

With tetracycline-induced and un-induced SMOXP9 cell lines transformed with constructs for RNAi expression, parasite growth was observed over the course of 7 days. The cultures of three clones were counted every day and diluted with SDM79 media to a concentration of $2x10^6$ cells/mL. The diagrams show theoretical cell density if the cells had not been diluted, by summing up the growth of every day.

The first growth curve showed a small growth defect, starting after 72 hours (Figure 16). Western blot analysis of samples taken every second day proved that p3030 was indeed down regulated (Figure 18).

The growth phenotype observed in the first growth curve was not reproducible in the second growth curve (Figure 17). This might be due to leakiness of the cell lines.

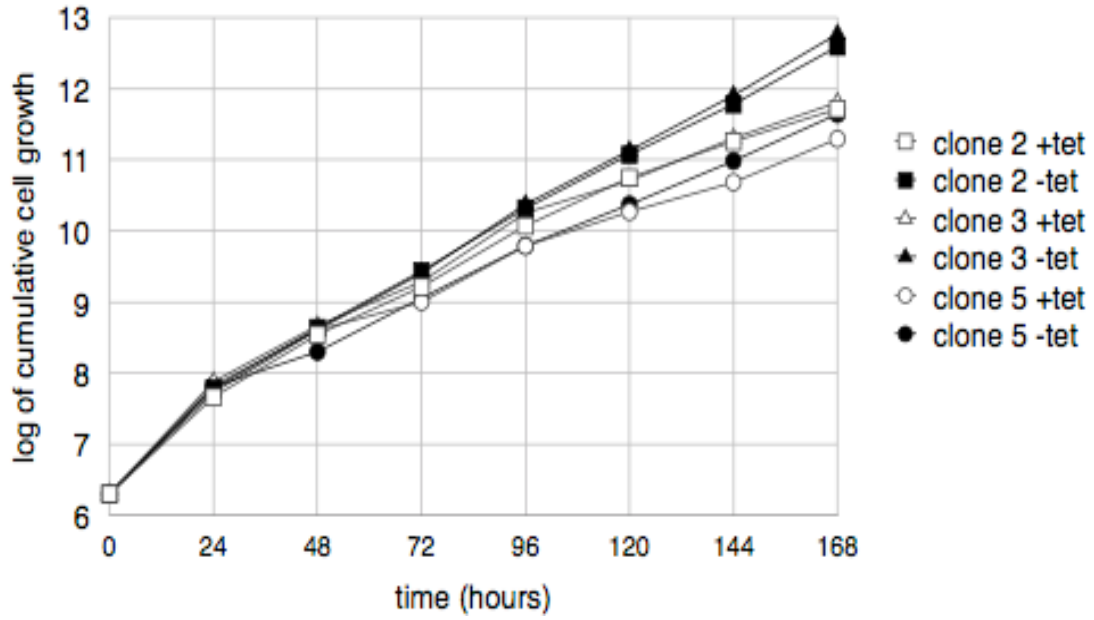

Figure 16. Growth curve of cells transfected with lhRNAi targeting for p3030, comparing non-induced cell lines to cell lines induced with tetracycline

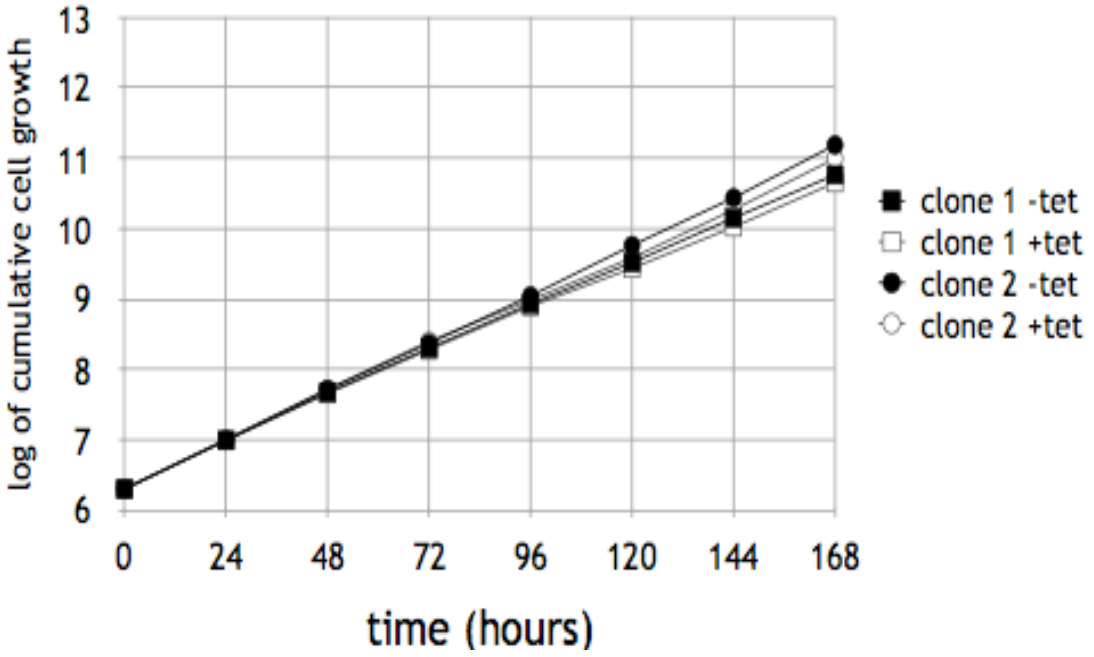

Figure 17. Growth curve of cells transfected with lhRNAi targeting for p3030 and C-terminal in-situ tagged with V5 of p3030, comparing non-induced cell lines to cell lines induced with tetracycline

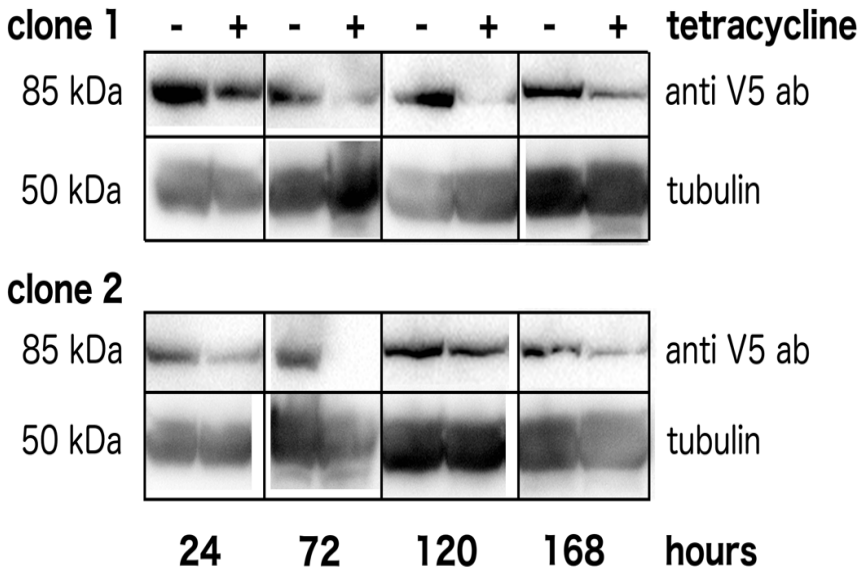

Figure 18. Western blot depicting downregulation of p3030 in a growth curve of uninduced cell lines (-) and induced (+) cells with tetracycline. $5x10^5$ cells are loaded per lane and tubulin is used as a loading control. The protein disappears after 72 hours and reappears after 120 hours.

5. Discussion

C-terminally tagged p4870 was located in the insoluble phase of the crude cell fractionation. In conjunction with structural similarities to transmembrane proteins and the high probability of transmembrane domains, it seems very likely that p4870 is a membrane-associated protein. RNAi knockdown of p4870 did not result in a phenotype, therefore we hypothesize that p4870 is not crucial for cell growth of procyclic *T. brucei.*

TrypTagDB localized p3030 in the mitochondria. This would immediately suggest itself, as the homolog in yeast Hsp78 strictly mitochondrial. However, half of the bioinformatics softwares used predicted the localization of p3030 in the mitochondria while, the other half did not. When p3030 was in-situ tagged with V5 at the C-terminus it was localized in the cytosol and in the mitochondria. *T. brucei* genome encodes for an annotated Hsp104 under the accession number Tb927.2.5980. The localization of Hsp78 in the cytosol in the presence of a Hsp104 ClpB homolog is not reported in any other organism.

The RNAi experiment of p3030 showed a slight phenotype. This indicates that the protein is relatively important for a normal growth. The slight phenotype, at first might suggest that p3030 is not highly important in the procyclic stage, however, its reappearance after 120 hours of induction with tetracyclin could suggest an acquired resistance against RNAi. This phenomenon concedes importance to the protein for the studied form of the parasite. Homologs of ClpB are known to resolublize aggregates that form in response to stress. Possibly, p3030 becomes of bigger importance in the response of *T. brucei* to stress induced by transformation of one life stage to the other.

Live imaging of p4870 and p3030 tagged with N-terminal mNeonGreen by TrypTag predicted the location of both proteins in the mitochondria. This finding could not be replicated by tagging of the proteins of interest with V5. The discrepancies between the findings of the live imaging approach of TrypTag and the endogenous tagging with V5 may indicate an artifact in the TrypTag project, which has to be examined further. The differences in localisation with tags at different ends of the protein suggest that mitochondrial localisation is indeed the real localisation of the protein. It should be remembered that mitochondrial targeting signals are found at the N-terminus of mitochondrially-localised proteins, therefore the inclusion of a tag at this location will block the mitochondrial tranlocation machinery from recognizing the target for translocation (Kunze and Berger, 2015).

On the other hand, p3030, as a putative ClpB protease localized to mitochondria and cytosol poses an interesting evolutionary adaptation. It has been hypothesized, that Hsp104 and Hsp78 in yeast share common clients, that are solubilized in the cytosol by Hsp104 and refolded upon translocation to the mitochondria by Hsp78 (Erives and Fassler, 2015). Loss of these common clients at the start of animal lineage as a result of the reduction of biosynthetic capacities, led to the loss of ClpBs in animals (Erives and Fassler, 2015). *T. brucei* may still possess some of these biosynthetic pathways. Though this result may originate on high turnover rates of the protein, in traffic from the cytosol to the mitochondria, this is only a speculation. The localization of p3030 in the cytosol, still presents a mystery. Leakage of the protein to the cytosol from a broken mitochondrion during the crude fractionation seems unlikely, as mtHsp70, the mitochondrial marker, did not localize in the cytosol in this experiment. It could be possible that common clients of Hsp78 and Hsp104 in *T. brucei* posses unique pathways and therefore require more careful supervision by more than one homolog of ClpB.

6. Summary

The main goal of this thesis was to localize genes Tb927.11.4870 and Tb927.2.3030 in *Trypanosoma brucei.* Both of these proteins were localized in the mitochondria in the results of TrypTag. The localization of the genes in the mitochondria would have proven the reproducibility of these findings.

However, when p4870 was tagged with V5 at its C-terminus by in-situ tagging using the long primer approach, it did not localize in the mitochondria. Immunofluorescence microscopy showed a signal for p4870 all over the cell. In conjunction with the localization of 4870 in the insoluble fraction in the cell fractionation, it could indicate that p4870 is localized on the cell membrane.

p3030, that was in-situ tagged with V5 at the C-terminus was localized in the cytosol and in the mitochondria.

The different localization by in-situ tagging with V5 and mNG, could indicate the presence of an artifact in the later approach.

Knockdown studies of p3030 with RNAi showed only a slight growth phenotype. Unfortunately, this could not be reproduced, as the cell lines might have developed a resistance towards RNAi.

7. References

AB, N. M. 2014. *The 2006 Nobel Prize in Physiology or Medicine - Advanced Information* [Online]. Available: http://www.nobelprize.org/nobel_prizes/medicine/laureates/2006/advanced.html [Accessed 12.05. 2018].

AMM, I., SOMMER, T. & WOLF, D. H. 2014. Protein quality control and elimination of protein waste: The role of the ubiquitin–proteasome system. *Biochimica et Biophysica Acta (BBA) - Molecular Cell Research,* 1843**,** 182-196.

ARHIN, G. K., SHEN, S., ULLU, E. & TSCHUDI, C. 2004. A PCR-Based Method for Gene Deletion and Protein Tagging in Trypanosoma brucei. *In:* MELVILLE, S. E. (ed.) *Parasite Genomics Protocols.* Totowa, NJ: Humana Press.

ASLETT, M., AURRECOECHEA, C., BERRIMAN, M., BRESTELLI, J., BRUNK, B. P., CARRINGTON, M., DEPLEDGE, D. P., FISCHER, S., GAJRIA, B., GAO, X., GARDNER, M. J., GINGLE, A., GRANT, G., HARB, O. S., HEIGES, M., HERTZ-FOWLER, C., HOUSTON, R., INNAMORATO, F., IODICE, J., KISSINGER, J. C., KRAEMER, E., LI, W., LOGAN, F. J., MILLER, J. A., MITRA, S., MYLER, P. J., NAYAK, V., PENNINGTON, C., PHAN, I., PINNEY, D. F., RAMASAMY, G., ROGERS, M. B., ROOS, D. S., ROSS, C., SIVAM, D., SMITH, D. F., SRINIVASAMOORTHY, G., STOECKERT, J. C. J., SUBRAMANIAN, S., THIBODEAU, R., TIVEY, A., TREATMAN, C., VELARDE, G. & WANG, H. 2010. TriTrypDB: a functional genomic resource for the Trypanosomatidae. *Nucleic Acids Research,* 38**,** D457-D462.

BABOKHOV, P., SANYAOLU, A. O., OYIBO, W. A., FAGBENRO-BEYIOKU, A. F. & IRIEMENAM, N. C. 2013. A current analysis of chemotherapy strategies for the treatment of human African trypanosomiasis. *Pathog Glob Health,* 107**,** 242-52.

BANNAI, H., TAMADA, Y., MARUYAMA, O., NAKAI, K. & MIYANO, S. 2002. Extensive feature detection of N-terminal protein sorting signals. *Bioinformatics,* 18**,** 298-305.

BENDER, T., BRADSHAW, I., FRANKEN, S., BAITZEL, C. & VOOS, W. 2011. *Mitochondrial enzymes are protected from stress-induced aggregation by mitochondrial chaperones and the Pim1/LON protease*.

CALDWELL, G. A., CAO, S., SEXTON, E. G., GELWIX, C. C., BEVEL, J. P. & CALDWELL, K. A. 2003. Suppression of polyglutamine-induced protein aggregation in Caenorhabditis elegans by torsin proteins. *Hum Mol Genet,* 12**,** 307-19.

CLAROS, M. G. & VINCENS, P. 1996. Computational method to predict mitochondrially imported proteins and their targeting sequences. *Eur J Biochem,* 241**,** 779-86.

DEAN, S., SUNTER, J., WHEELER, R. J., HODKINSON, I., GLUENZ, E. & GULL, K. 2015. A toolkit enabling efficient, scalable and reproducible gene tagging in trypanosomatids. *Open Biology,* 5.

DEAN, S., SUNTER, J. D. & WHEELER, R. J. 2017. TrypTag.org: A Trypanosome Genome-wide Protein Localisation Resource. *Trends in Parasitology,* 33**,** 80-82.

DOUGAN, D. A. 2013. *Regulated Proteolysis in Microorganisms*, Springer Netherlands.

EMANUELSSON, O., NIELSEN, H., BRUNAK, S. & VON HEIJNE, G. 2000. Predicting subcellular localization of proteins based on their N-terminal amino acid sequence. *J Mol Biol,* 300**,** 1005-16.

ERIVES, A. J. & FASSLER, J. S. 2015. Metabolic and Chaperone Gene Loss Marks the Origin of Animals: Evidence for Hsp104 and Hsp78 Chaperones Sharing Mitochondrial Enzymes as Clients. *PLoS ONE,* 10**,** e0117192.

GIBSON, D. G., YOUNG, L., CHUANG, R.-Y., VENTER, J. C., HUTCHISON III, C. A. & SMITH, H. O. 2009. Enzymatic assembly of DNA molecules up to several hundred kilobases. *Nature Methods,* 6**,** 343.

GLOVER, J. R. & LINDQUIST, S. 1998. Hsp104, Hsp70, and Hsp40. *Cell,* 94**,** 73-82.

GOMI, M., SONOYAMA, M. & MITAKU, S. 2004. High performance system for signal peptide prediction: SOSUIsignal. *Chem-Bio Informatics Journal,* 4**,** 142-147.

HANSON, P. I. & WHITEHEART, S. W. 2005. AAA+ proteins: have engine, will work. *Nature Reviews Molecular Cell Biology,* 6**,** 519.

HOGLUND, A., DONNES, P., BLUM, T., ADOLPH, H. W. & KOHLBACHER, O. 2006. MultiLoc: prediction of protein subcellular localization using N-terminal targeting sequences, sequence motifs and amino acid composition. *Bioinformatics,* 22**,** 1158-65.

KÄLL, L., KROGH, A. & SONNHAMMER, E. L. L. 2007a. Advantages of combined transmembrane topology and signal peptide prediction—the Phobius web server. *Nucleic Acids Research,* 35**,** W429-W432.

KÄLL, L., KROGH, A. & SONNHAMMER, E. L. L. 2007b. Advantages of combined transmembrane topology and signal peptide prediction—the Phobius web server. *Nucleic Acids Research,* 35**,** W429-W432.

KUNZE, M. & BERGER, J. 2015. The similarity between N-terminal targeting signals for protein import into different organelles and its evolutionary relevance. *Frontiers in Physiology,* 6**,** 259.

LIBEREK, K., LEWANDOWSKA, A. & ZIETKIEWICZ, S. 2008. Focus Quality Control

Chaperones in control of protein disaggregation. *The EMBO Journal,* 27**,** 328-335.

LOPES, A. H. 2010. Trypanosomatids: Odd Organisms, Devastating Diseases. *The Open Parasitology Journal,* 4**,** 30-59.

MATTHIAS SCHMITT, W. N., THOMAS LANGER 1996. The molecular chaperone Hsp78 confers compartment-specific thermotolerance to mitochondria. *The Journal of Cell Biology,* 134**,** 1375-1386.

MCALLASTER, M. R., SINCLAIR-DAVIS, A. N., HILTON, N. A. & GRAFFENRIED, C. 2016. *A unified approach towards Trypanosoma brucei functional genomics using Gibson assembly*.

NGÔ, H., TSCHUDI, C., GULL, K. & ULLU, E. 1998. Double-stranded RNA induces mRNA degradation in Trypanosoma brucei. *Proceedings of the National Academy of Sciences,* 95**,** 14687-14692.

PARSONS, M. 2004. Glycosomes: parasites and the divergence of peroxisomal purpose. *Molecular Microbiology,* 53**,** 717-724.

PEÑA-DIAZ, P., VANCOVÁ, M., RESL, C., C FIELD, M. & LUKEŠ, J. 2017. *A leucine aminopeptidase is involved in kinetoplast DNA segregation in Trypanosoma brucei*.

PETERSEN, T. N., BRUNAK, S., VON HEIJNE, G. & NIELSEN, H. 2011. SignalP 4.0: discriminating signal peptides from transmembrane regions. *Nature Methods,* 8**,** 785.

REQUENA, J. M., MONTALVO, A. M. & FRAGA, J. 2015. Molecular Chaperones of Leishmania: Central Players in Many Stress-Related and -Unrelated Physiological Processes. *BioMed Research International,* 2015**,** 301326.

SINGH, A. & GROVER, A. 2010. Plant Hsp100/ClpB-like proteins: poorly-analyzed cousins of yeast ClpB machine. *Plant Molecular Biology,* 74**,** 395-404.

SINGH, A., SINGH, U., MITTAL, D. & GROVER, A. 2010. Genome-wide analysis of rice ClpB/HSP100, ClpC and ClpD genes. *BMC Genomics,* 11**,** 95-95.

SÖDING, J. 2005. Protein homology detection by HMM–HMM comparison. *Bioinformatics,* 21**,** 951-960.

VERNER, Z., BASU, S., BENZ, C., DIXIT, S., DOBAKOVA, E., FAKTOROVA, D., HASHIMI, H., HORAKOVA, E., HUANG, Z., PARIS, Z., PENA-DIAZ, P., RIDLON, L., TYC, J., WILDRIDGE, D., ZIKOVA, A. & LUKES, J. 2015. Malleable mitochondrion of Trypanosoma brucei. *In:* JEON, K. W. (ed.) *International Review of Cell and Molecular Biology.* 2015/02/25 ed.

WANG, Y., SATOH, A., WARREN, G. & MEYER, H. H. 2004. VCIP135 acts as a deubiquitinating enzyme during p97-p47-mediated reassembly of mitotic Golgi fragments. *J Cell Biol,* 164**,** 973-8.

WANG, Z., MORRIS, J. C., DREW, M. E. & ENGLUND, P. T. 2000. Inhibition of Trypanosoma brucei Gene Expression by RNA Interference Using an Integratable Vector with Opposing T7 Promoters. *Journal of Biological Chemistry,* 275**,** 40174-40179.

ZIMMERMANN, L., STEPHENS, A., NAM, S.-Z., RAU, D., KÜBLER, J., LOZAJIC, M., GABLER, F., SÖDING, J., LUPAS, A. N. & ALVA, V. 2017. A Completely Reimplemented MPI Bioinformatics Toolkit with a New HHpred Server at its Core. *Journal of Molecular Biology*.